Optimal Operation of Residential High Performance Water Heater for Reduction of Electricity Cost and Peak Demand Through Field Validation[1]

Guodong Liu, Oak Ridge National Laboratory
Robert Smith, Oak Ridge National Laboratory
Helia Zandi, Oak Ridge National Laboratory

ABSTRACT

Water heating accounts for about 18% of a typical US home's energy use. Modern water heaters have enabled control options through APIs, offering customers the opportunity to reduce their energy cost and peak demand by dynamically adjusting settings. A water heater's capacity to store energy using its storage tank makes it an asset for peak demand reduction and energy cost savings. For this reason, a mixed-integer linear programming model is proposed to minimize the energy cost of a high-performance water heater while also reducing the peak demand of the residential household under a time-of-use utility rate by dynamically changing the water heater's running mode. Specifically, a multi-objective optimization model is formulated to determine the mode settings of the water heater considering hot water use, time-of-use rate, and peak demand limit of the residential household. The mode settings are associated with different dead bands of water temperature for triggering on/off action of the heat pump and heating element. A 66-gal hybrid electric high performance water heater was used for numerical simulation and practical experiments. The simulation results were well aligned with measurements of practical experiments, validating the soundness of the thermodynamic model. In addition, reductions of energy cost, enabling affordability, and reducing peak demand are demonstrated. The research team also developed a software framework with dashboards to automatically and continuously monitor and manage devices.

Introduction

Water heating accounts for about 18% of a typical US home's energy use and is typically a home's second largest energy expense (EIA 2009). A water heater can store energy using its storage tank, which behaves like an energy storage tool and provides flexibility in its energy consumption. Modern water heaters enable control options through APIs, allowing customers to reduce their energy cost and providing utilities with various ancillary services (e.g., peak reduction, frequency response reserve) by dynamically adjusting water heater operation. Various optimization models for hybrid water heater control have been proposed and validated to reduce residential energy costs while preserving users' comfort under dynamic electricity rates (Pardiñas et al. 2023, Bursill and Cruickshank 2015). The coordinated operation of water heaters, rooftop PV, and battery energy storage systems in residential households has been demonstrated

---

[1] Notice: This manuscript has been authored by UT-Battelle, LLC, under contract DE-AC05-00OR22725 with the US Department of Energy (DOE). The US government retains and the publisher, by accepting the article for publication, acknowledges that the US government retains a nonexclusive, paid-up, irrevocable, worldwide license to publish or reproduce the published form of this manuscript, or allow others to do so, for US government purposes. DOE will provide public access to these results of federally sponsored research in accordance with the DOE Public Access Plan (https://www.energy.gov/doe-public-access-plan).

using mixed-integer linear programming (MILP) (Clift et al. 2023). Advanced demand response value streams (e.g., frequency reserve and voltage regulation) for water heaters in renewable-rich electricity markets have been investigated in Yinyan and Yildiz (2025).

Water heaters are traditionally controlled by directly turning the heating elements on or off or by changing the temperature set point. Aggregated load control systems that account for direct on/off control of domestic electric water heaters have been developed to mitigate unbalanced power caused by intermittent renewable generation and to support demand response programs, as described in Shad et al. (2017). A model predictive control (MPC) of residential building water heaters has been proposed in Starke et al. (2020) and Hall et al. (2022) to reduce the electricity cost to consumers by dynamically changing water heater temperature set points. Direct control of residential water heaters requires access to data and control authority of the utility, which raises privacy concerns; thus, vendors are starting to define different operating modes for sophisticated control of water heaters. For example, Tsybina et al. (2023) proposes a control method for residential water heaters to reduce peak demand by dynamically adjusting the manufacturer-defined operating modes.

Hybrid high performance water heaters (HPWHs) have become popular in recent years and are increasingly being deployed because of their improved energy use. Unlike a standard electric water heater, which uses only electric elements to heat tank water, the hybrid HPWH has both a heat pump and an electric element to provide dual heating options. The heat pump is far more efficient but has a much smaller capacity than that of the electric heating element. However, the electric element's larger capacity enables faster recovery of water temperature during periods of high hot water consumption. Thus, to improve the overall efficiency of the HPWH, the heat pump should be used as the primary heating source with the electric element serving as a backup. One study (Jin, Maguire, and Christensen 2014) proposed an MPC framework that dynamically increases use of the heat pump and reduces use of electric elements for energy savings by learning the household's hot water consumption patterns. An optimization model is formulated to find the optimal setpoint profile for the heat pump and element that minimizes the weighted sum of energy consumption and thermal comfort over the prediction horizon. Another economic MPC of an HPWH was proposed in Mande et al. (2022) using a graph-based control framework that could modularize the problem formulation. For utilities, Stübs, Grant, and Nordman (2024) and Grant et al. (2023) separately studied the capability of shaping load profiles and stabilizing the grid by balancing demand and supply through price-responsive control of HPWHs. Model-free controls of water heaters using various data-driven machine learning algorithms were proposed in Ayoola et al. (2025) and Amasyali et al. (2021). Nevertheless, dynamic control of HPWHs is realized by directly controlling the on/off heating options or by changing the temperature set point.

The existing research mostly controls the electric or heat pump water by turning the equipment on or off, or by using a temperature set point in a continuous range. However, most water heaters available in the market cannot perform these actions or change settings remotely. Instead, they receive demand response commands to change the manufacture-defined operating modes (e.g., *Shed*, *Normal*, and *Load*). In view of this gap, a MILP-based optimization model is formulated to determine the optimal mode settings of the water heater by considering the residential household's hot water use, time-of-use (TOU) rate, and peak demand limit. Both numerical simulation and field deployment have been performed to validate the effectiveness of the proposed control, and reductions in electricity cost and peak demand have been demonstrated. Following are the main contributions of this paper:

- The paper proposes an optimal control of an HPWH that considers hot water use, TOU rate, and peak demand limit of the residential household. The water heater is controlled by dynamically selecting the manufacture-defined operating modes instead of directly turning the heating options on/off or changing the temperature set points, thus preserving consumer privacy.
- The problem of determining the optimal mode settings of the water heater is formulated as a MILP, which could be efficiently solved by various open-source solvers (e.g., COIN-OR Branch and Cut solver).

The Problem Formulation section introduces the proposed MILP-based optimization for optimal HPWH control. Results of case studies and field deployments are presented in the sections titled Case Studies and Field Validation Results, respectively. The last section presents concluding remarks.

Problem Formulation

Heat Pump Water Heater Modeling

We established a two-node HPWH model with an electric element in the upper node and a heat pump in the lower node based on Amasyali et al. (2021). Figure 1 illustrates the model. The water tank is divided into two nodes—cold water is fed from the lower node, hot water is drawn from the upper node, and the subsequent vacant space is filled by water from the lower node. The temperature inside each node is assumed to be uniform, and heat is transferred between the lower and upper nodes by natural conduction and convection. Temperatures of the upper and lower nodes are formulated based on heat pump on/off, electric element on/off, hot water draw, heat loss through tank wall, and heat natural conduction and convection.

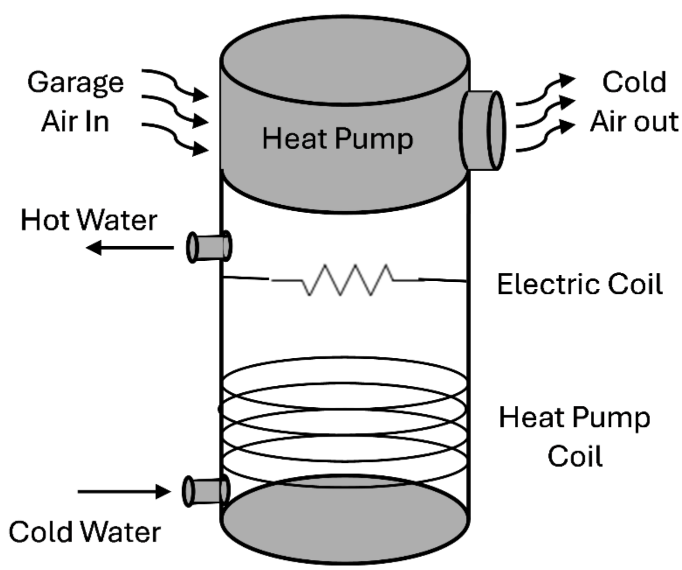

Figure 1. Diagram of an HPWH.

Objective Function

The objective function 1 includes three parts: (1) minimize the utility bill, (2) minimize the number of water heater mode changes to avoid frequent cycling, and (3) minimize the peak demand of the residential household. These three parts are unified into a single objective function by weighting factors W^C, W^M, and W^P.

$$\min\ W^C \sum_{t=1}^{N_T} \lambda_t P_t^T + W^M \sum_{t=1}^{N_T} Chg_t^{mode} + W^P P^P. \tag{1}$$

Constraints

Heat balance of each water tank node. The water tank is divided into 2 nodes. The heat pump is in the lower node ($j = 0$), and the heating element is in the upper node ($j = 1$). Cold water is fed from the lower node, whereas hot water is drawn from the upper node. The water temperature of a node for the next period depends on several factors: the node's water temperature at the current period, heat from the heat pump or electric element, natural conduction $\boldsymbol{Q_{tj}^{cond}}$ and convection $\boldsymbol{Q_{tj}^{conv}}$ of heat with adjacent nodes, heat loss through the tank wall, and the water draw W_t. The heat balances of the lower and upper nodes are formulated in (2) and (3), respectively.

$$T_{t+1,j} = T_{tj} + \frac{\Delta t}{C_j}\left[UA_j\left(T^A - T_{tj}\right) + W_t c_p\left(T^C - T_{tj}\right) + H_{HP} On_t^{HP} - Q_{tj}^{cond} - Q_{tj}^{conv}\right], j = 0, \tag{2}$$

$$T_{t+1,j} = T_{tj} + \frac{\Delta t}{C_j}\left[UA_j\left(T^A - T_{tj}\right) + W_t c_p\left(T_{t,0} - T_{tj}\right) + H_{EE} On_t^{EE} + Q_{tj}^{cond} + Q_{tj}^{conv}\right], j = 1. \tag{3}$$

The upper node temperature is assumed to be no lower than the lower node temperature. The constraint defined in (4) prevents the temperature of the lower node from being higher than or 10 °*F* lower than the temperature of the upper node.

$$T_{t,j+1} - \Delta T^{max} \leq T_{tj} \leq T_{t,j+1}\,. \tag{4}$$

Heat Conduction Between Nodes: Natural heat conduction occurs between the lower and upper nodes owing to temperature differences. Because the upper node temperature is no lower than the lower node temperature, $T_{t,j} - T_{t,j+1} \leq 0$, and $\boldsymbol{Q_{tj}^{cond}}$ is a nonpositive value. Heat conduction is presented in (5).

$$kS\left(T_{tj} - T_{t,j+1}\right)\Delta t \leq Q_{tj}^{cond} \leq 0. \tag{5}$$

Heat Convection Between Nodes: Heat convection occurs between the lower and upper nodes. The heat convection is limited by the heat input H_{HP} and happens only when $\boldsymbol{u_{tj}^{conv}}$ is 1, as in (6). The binary variable $\boldsymbol{u_{tj}^{conv}}$ indicates convection occurs in an upward direction.

$$0 \leq Q_{tj}^{conv} \leq H_{HP} u_{tj}^{conv}. \tag{6}$$

In addition, when heat convection takes place, the upper and lower nodes end up with the same temperature, as enforced by (7). Meanwhile, the lower node should not drop in temperature while using natural convection to transfer heat upward, as enforced by (8).

$$T_{t,j+1} - T_{tj} \leq M\left(1 - u_{tj}^{conv}\right). \tag{7}$$

$$T_{tj} - T_{t,j+1} \leq M\left(1 - u_{tj}^{conv}\right). \tag{8}$$

Constraint of Mode Selection: The HPWH can be operated in different modes—*Shed*, *Normal*, and *Load*. Only one mode (i.e., 1) can be active at any time, as enforced by (9).

$$M_t^{shed} + M_t^{normal} + M_t^{load} = 1\,. \tag{9}$$

Based on the selected operating mode, the lower temperature limit of the dead band for turning on the heat pump can be formulated as (10).

$$T_t^{limit} = T^{set} - M_t^{shed} D^{shed} - M_t^{normal} D^{normal} - M_t^{load} D^{load} = 1\,. \tag{10}$$

Constraint of Heat Pump On/Off Control:

The heat pump is in the bottom node of the water heater. Based on the selected operating mode, if the temperature of the bottom node is lower than the $\boldsymbol{T_t^{limit}}$, the binary indicator for turning on the heat pump is triggered (i.e., $\underline{\boldsymbol{B_t^{HP}}}$ will be 1). If the bottom node temperature reaches the set point T^{set}, the binary indicator for turning off the heat pump is triggered (i.e., $\overline{\boldsymbol{B_t^{HP}}}$ will be 1). Otherwise, it will be 0. These constraints are enforced by (11) and (12).

$$\left(T_t^{limit} - T_{t,0}\right)/M \leq \underline{B_t^{HP}} \leq 1 + \left(T_t^{limit} - T_{t,0}\right)/M\,, \tag{11}$$

$$\left(T_{t,0} - T^{set}\right)/M \leq \overline{B_t^{HP}} \leq 1 + \left(T_{t,0} - T^{set}\right)/M\,. \tag{12}$$

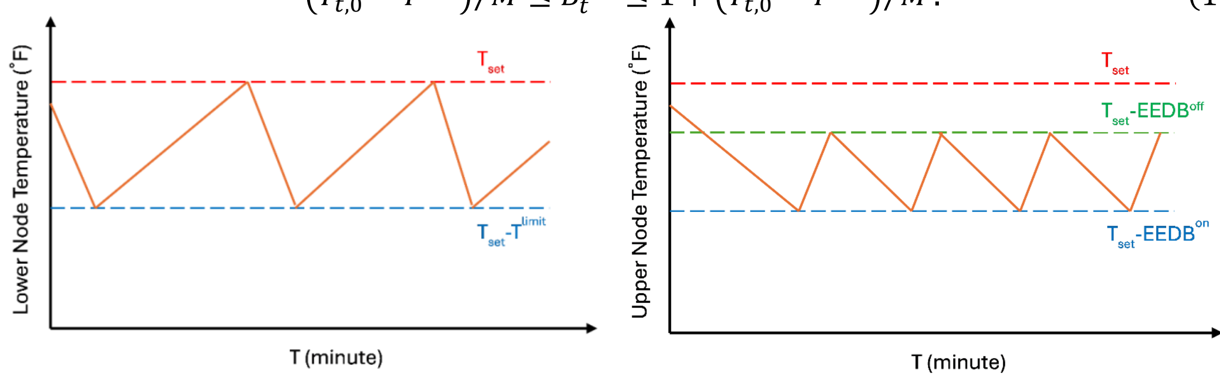

(a) (b)

Figure 2. Control logic of the HPWH: (a) heat pump and (b) electric element.

The basic control logic of the heat pump is illustrated in Figure 2a. As can be seen, once the heat pump is turned on, it will be kept on until the bottom node temperature reaches the set point T^{set}, and then it will be turned off. The heat pump will be turned on again when the bottom node temperature gets below T_t^{limit}. Therefore, whenever the lower temperature limit of the dead band for turning on the heat pump is triggered, $\underline{B_t^{HP}}$ will be 1 and the heat pump will be turned on (i.e., On_t^{HP} will be 1). On the other hand, whenever the upper temperature limit of the dead band for the heat pump is triggered, $\overline{B_t^{HP}}$ will be 1, and the heat pump will be turned off (i.e., On_t^{HP} will be 0). This logic may be expressed as (13).

$$\underline{B_t^{HP}} \leq On_t^{HP} \leq 1 - \overline{B_t^{HP}}\,. \tag{13}$$

When neither the lower nor upper temperature dead band of the heat pump is triggered, the heat pump will keep the same status as that of the previous time step. This logic may be expressed as (14).

$$On_{t-1}^{HP} - \underline{B_t^{HP}} - \overline{B_t^{HP}} \leq On_t^{HP} \leq On_{t-1}^{HP} + \underline{B_t^{HP}} + \overline{B_t^{HP}}\,. \tag{14}$$

Constraint of Heating Element On/Off Control: The heating element is in the upper node of the water heater. If the water temperature of the upper node is below $T^{set} - D^{on}$, which is the lower temperature dead band of turning on the heating element, the binary indicator for turning on the electric element is triggered (i.e., $\underline{\boldsymbol{B_t^{EE}}}$ will be 1). If the water temperature of the upper node reaches $T^{set} - D^{off}$, which is the upper temperature dead band of turning off the electric element, the binary indicator for turning off the heating element is triggered (i.e., $\overline{\boldsymbol{B_t^{EE}}}$ will be 1). Otherwise, it will be 0. These constraints are enforced by (15) and (16).

$$\frac{(T^{set} - D^{on}) - T_{t,1}}{M} \leq \underline{B_t^{EE}} \leq 1 + \frac{(T^{set} - D^{on}) - T_{t,1}}{M}, \tag{15}$$

$$\frac{T_{t,1} - (T^{set} - D^{off})}{M} \leq \overline{B_t^{EE}} \leq 1 + \frac{T_{t,1} - (T^{set} - D^{off})}{M}. \tag{16}$$

The basic control logic of the heating element is like that of the heat pump, as illustrated in Figure 2b. Once the heating element is turned on, it will be kept on until the upper node temperature reaches $T^{set} - D^{off}$, then it will be turned off. It will be turned on again when the upper node temperature drops below $T^{set} - D^{on}$. Therefore, whenever the lower temperature dead band of the electric element is triggered, $\underline{B_t^{EE}}$ will be 1, and the heating element will be turned on (i.e., On_t^{EE} will be 1). On the other hand, when the upper temperature dead band of the heating element is triggered, $\overline{B_t^{EE}}$ will be 1, and the heating element will be turned off (i.e., On_t^{EE} will be 0). This logic may be expressed as (17).

$$\underline{B_t^{EE}} \leq On_t^{EE} \leq 1 - \overline{B_t^{EE}}\,. \tag{17}$$

When neither the lower node nor upper node temperature dead band of the heating element is triggered, the heating element keeps the same status as that of the previous time step. This logic may be expressed as (18).

$$On_{t-1}^{EE} - \underline{B_t^{EE}} - \overline{B_t^{EE}} \leq On_t^{EE} \leq On_{t-1}^{EE} + \underline{B_t^{EE}} + \overline{B_t^{EE}} . \quad (18)$$

The heat pump and heating element control logics are shown in Figure 2. Note that the temperature dead band of the heating element in the upper node is much narrower than that of the heat pump in the lower node, which limits water temperature deviations in the upper node, guaranteeing user comfort.

Constraint of Identifying Mode Change: When any mode change occurs, one mode is deactivated (i.e., the corresponding mode variable is changed to 0). Meanwhile, another mode must be activated (i.e., the corresponding mode variable is changed to 1). For this reason, only the change of the mode being activated must be captured, as in (19)– (21).

$$Chg_t^{load} \geq M_t^{load} - M_{t-1}^{load} , \quad (19)$$

$$Chg_t^{normal} \geq M_t^{normal} - M_{t-1}^{normal} , \quad (20)$$

$$Chg_t^{shed} \geq M_t^{shed} - M_{t-1}^{shed} . \quad (21)$$

The overall system mode change takes place when any of the specific modes changes. This relationship may be expressed as (22).

$$Chg_t^{mode} = Chg_t^{load} + Chg_t^{normal} + Chg_t^{shed} . \quad (22)$$

Constraint of Total Power Consumption: The total power consumption of the HPWH includes the power consumption of the heat pump and the heating element, as in (23).

$$P_t^{WH} = On_t^{HP} P^{HP} + On_t^{EE} P^{EE} . \quad (23)$$

Considering the charging of electric vehicle and other household loads, the total power of the residential household is limited, as in (24).

$$P_t^{WH} + P_t^{EV} + P_t^{OL} = P_t^T \leq P^P . \quad (24)$$

Case Studies

Test Settings

The simulation schedules the HPWH to run for 6 hours at 10-minute intervals. The goals are to minimize the energy bill and minimize the household peak demand. Thus, the weighting factors W_{cost}, W_{mode}, and W_{peak} are set as 1, 0.001, and 0.01, respectively. The utility rate and amount of hot water draw are shown in Figures 3a and 3b, respectively. Note that the simulation is based on a 6-hour time horizon with 10-minute time resolution, so the horizontal axis is 36 10-minute intervals.

Besides HPWHs, electric vehicle charging and other residential household loads are also considered. A constant 10 kW charging power for an electric vehicle is constantly assumed, whereas other residential loads are between 0 and 2.4 kW. Both loads are shown in Figure 4. The optimization is programmed in Python and solved using an open-source MILP solver, the COIN-OR Branch and Cut solver (COIN-OR 2022). The solution time of each case is less than 15 s on a 2.66 GHz Windows-based PC with 4 GB of RAM.

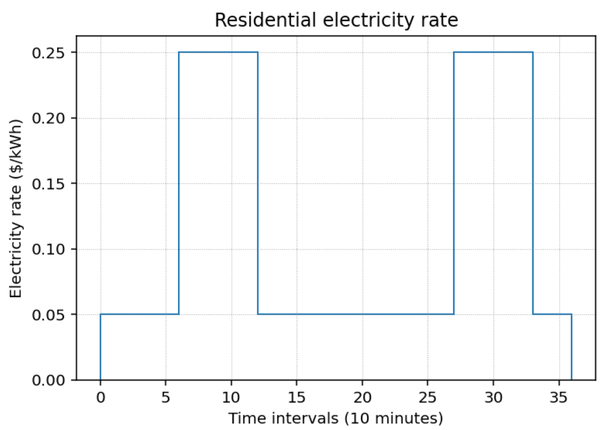

(a)

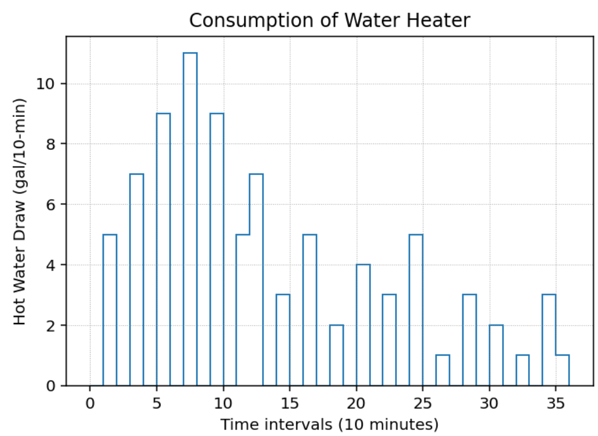

(b)

Figure 3. (a) Residential TOU rate and (b) hot water draw schedule.

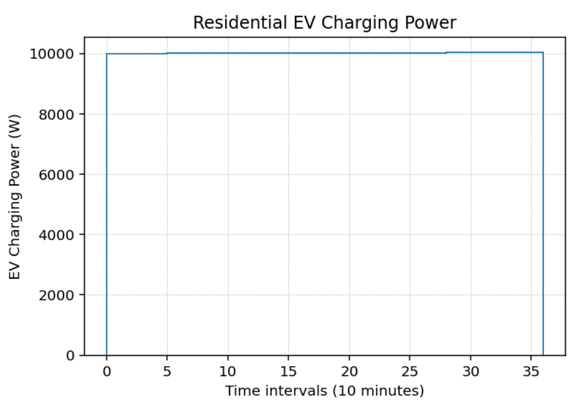

(a)

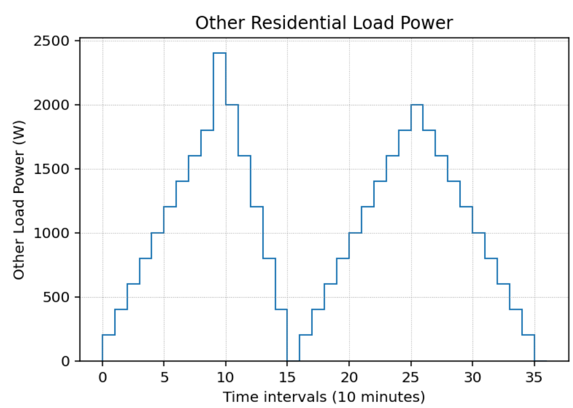

(b)

Figure 4. (a) Electric vehicle charging power and (b) other residential load power.

Base Case

In the base case study, no optimization is used, and the HPWH is consistently set as a *Normal* mode. For the 6-hour scheduling horizon, the water temperature of the lower and upper water heater nodes is shown in Figure 5. The temperature of both nodes decreases significantly when large amounts of water are drawn, as seen in Figure 5. In addition, the water temperature deviation of the upper node is smaller than that of the lower node to guarantee user comfort. The total power consumption of the HPWH is shown in Figure 6a. Generally, the water heater turns on the heat pump (at time interval 8) and heating element (at time interval 10) until the water temperatures of the lower node and upper node get out of the dead bands. Otherwise, they are kept off. The total energy cost of the HPWH over the course of the 6 h test window is $1.07, and the peak load of the house is 17.3 kW, as shown in Figure 6b.

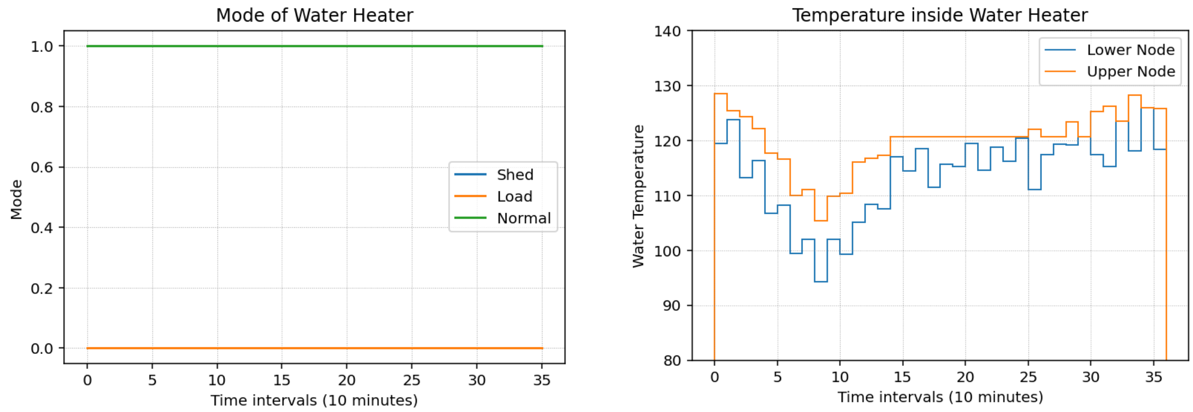

(a) (b)

Figure 5. (a) Operating mode and (b) water temperature of the HPWH in the base case.

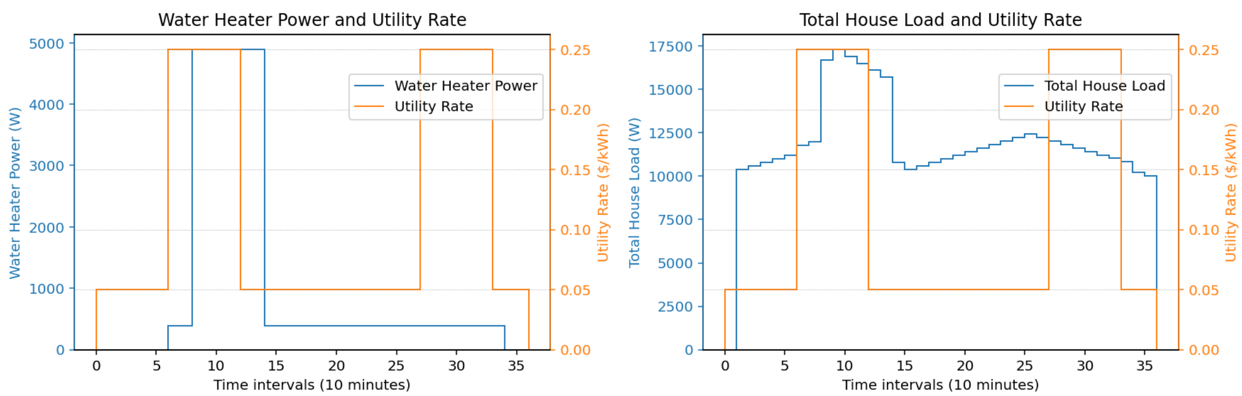

(a) (b)

Figure 6. Power consumption in the base case of (a) the HPWH and (b) the total household.

Optimized Case

The proposed optimization model for optimal HPWH scheduling is solved in this case. The solution is used to set the operating mode of the HPWH accordingly. The optimal operating mode for the 6-hour scheduling horizon is shown in Figure 7a, and the water temperature of the lower and upper water heater nodes is shown in Figure 7b. As can be seen, the temperature decreases of both nodes after large amounts of water have been reduced when compared with the base case. This reduction occurs primarily because the heat pump is turned on and the water is preheated before the large amount of water is drawn to avoid turning on the low-efficiency heating element. This approach improves and reduces the overall energy use of the HPWH.

The total power consumption of the HPWH is shown in Figure 8a. Generally, the water heater turns on the heat pump and heating element until the water temperature of the lower and upper nodes is out of the dead bands. However, the heat pump is turned on earlier (at time interval 3) by changing the operating mode from *Normal* to *Load* (i.e., the temperature dead band of the heat pump is narrowed to trigger turning on of the heat pump). As a result, the water tank is preheated and prepared for the large amounts of water to be drawn in time intervals 7 and 9. This delays turning on the heating element until time interval 10, thus mostly avoiding the peak price hours and peak household load. The running time of the low-efficiency heating element is also significantly reduced. The total energy cost of the HPWH is $0.71 (about a 33.64% reduction from the base case), and the peak load of the house is 16.9 kW (about a 2.31% reduction from the base case), as shown in Figure 8b. The water heater power consumption during the peak price hours has been reduced to 2.28 kWh (from 3.78 kWh in the base case, or about a 33.68% reduction).

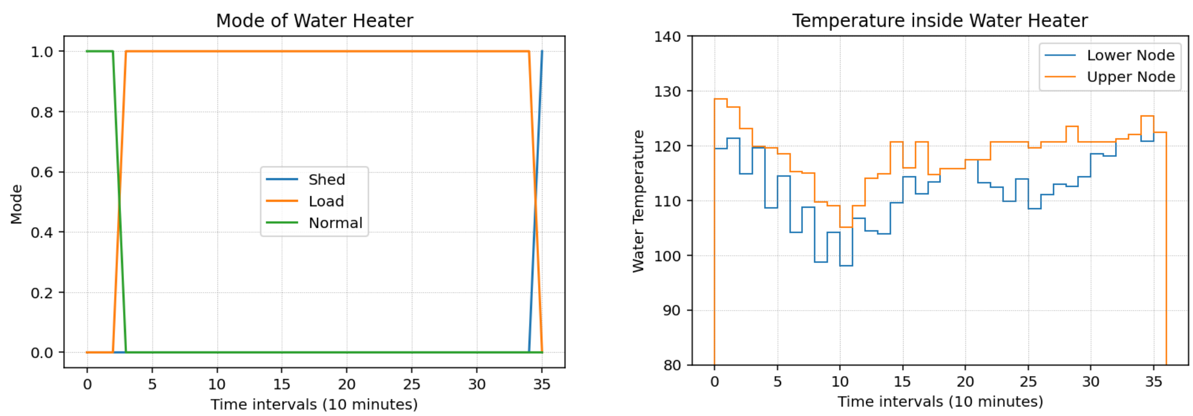

(a) (b)

Figure 7. (a) Operating mode and (b) water temperature of the HPWH in the optimized case.

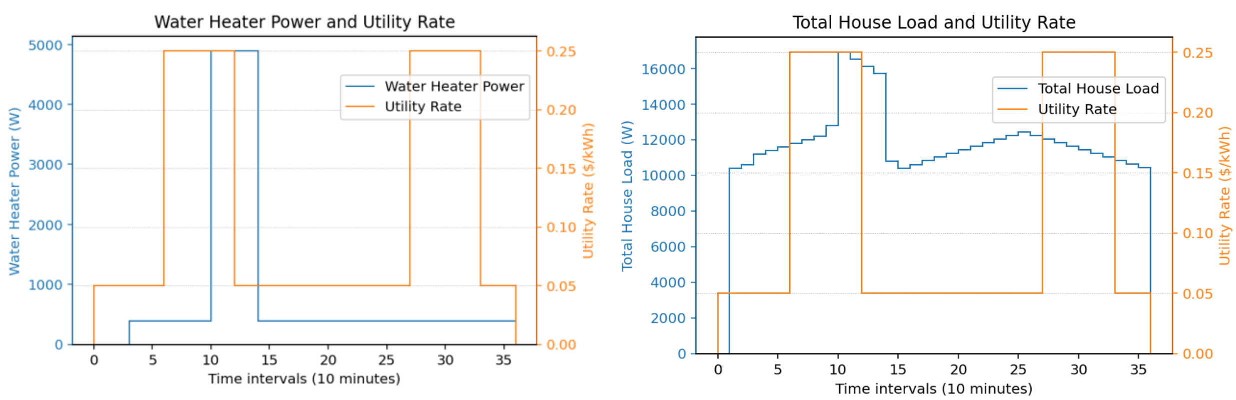

(a) (b)

Figure 8. Power consumption in the optimized case of (a) the HPWH and (b) the total household.

Field Validation Results

The software architecture for the field validation is based on the ACTIVE framework (Smith et al. 2025) to define the deployment as a series of ACTIVE style components as shown in Figure 9. These components include: 1) the algorithm described in previous section; 2) other components which communicate with one particular type of remote web servers or databases for sensor data collection, device control, and long-term data storage. Two collections of components, termed an environment, were used. One environment handled continuous data collection through regular scheduled queries to remote servers for each device, while the other ran the optimization algorithm once in the morning and dispatched the results one timestep at a time every 10 minutes during the control period.

The ACTIVE framework initializes a number of components and integrates them to enable data transference. Three components are responsible for communication with vendor specific water heater, electric vehicles, and data logger devices, while a fourth does the same to a database. The strategy components run logic to scrape data from the devices in one environment and to run the control algorithm and dispatch changes to the smart devices in the other. Live data is made available via web browser.

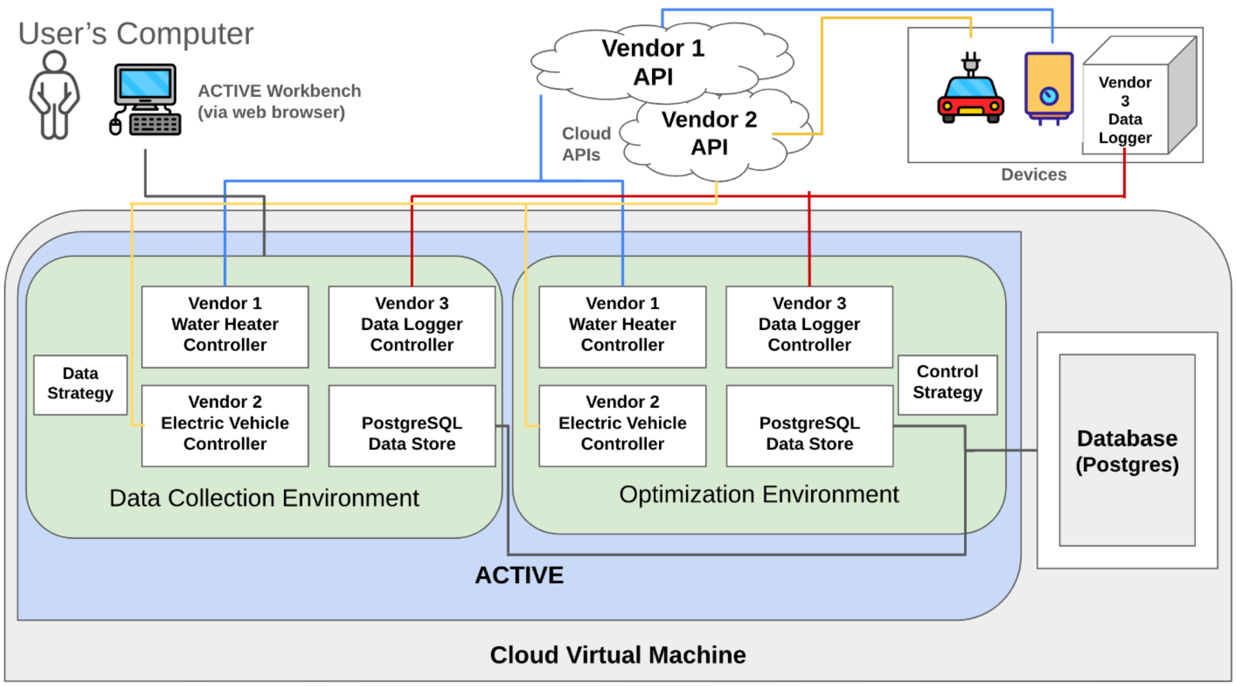

Figure 9. Diagram of the field validation software.

The HPWH is scheduled for 6 hours in the field validation test. The optimization results of mode selection are used to dispatch the mode of the water heater. The utility rate and amount of water drawn are the same as that shown in Figure 3, whereas the water temperature of the lower and upper nodes is shown in Figure 10. As can be seen in Figure 10, the water temperature drops to the minimum at time interval 10 after intensive water draws between time intervals 5 and 10. Then, the water temperature quickly recovers because the heating element turns on. Comparing the average temperature of tank water between the optimized simulation case and the field deployment case in Figure 11, the temperatures of the simulation and field deployment follow the same trend, indicating the soundness of the model. The difference could be due to inaccuracy of thermal parameters and the fluctuations of inlet cold water temperature and garage temperature.

The total power consumption of the HPWH in the field deployment is shown in Figure 12a. The water heater generally uses the heat pump first owing to its high efficiency. This occurs by changing the mode from *Normal* to *Load* at time interval 3 so that the heat pump will be turned on. As a result, the water tank is preheated and prepared for the coming large amounts of water drawn in time intervals 7 and 9. In this way, turning on the heating element is delayed until time interval 9, which largely avoids the peak price hours. The total electricity cost of the HPWH is about $0.93 (about a 13.08% reduction from the base case). The total load profile of the house is shown in Figure 12b. Although the peak load of the house is still 17.3 kW (the same as the base case), the water heater energy consumption during peak price hours has been reduced to 3.03 kWh (from 3.78 kWh in the base case, about a 19.84% reduction).

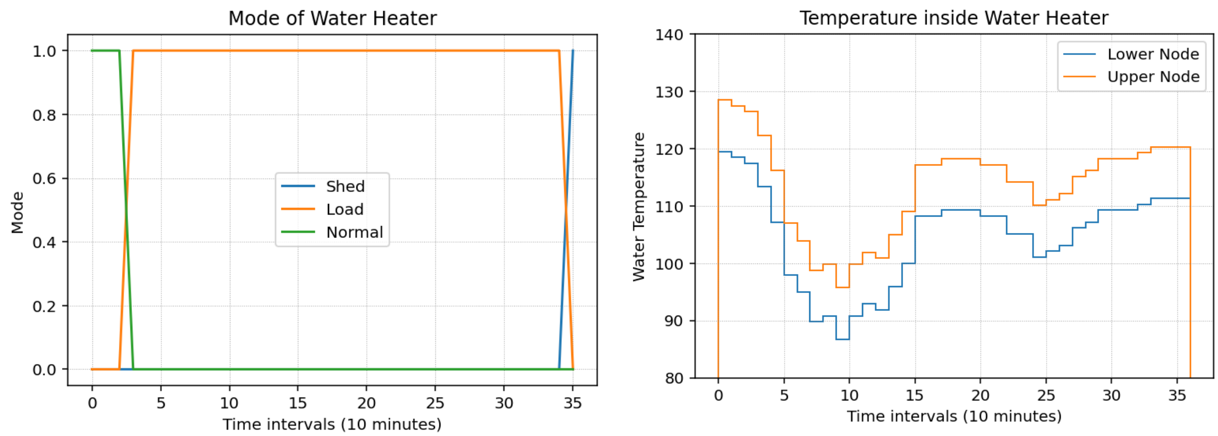

(a) (b)

Figure 10. (a) Operating mode and (b) water temperature of the HPWH in the field deployment case.

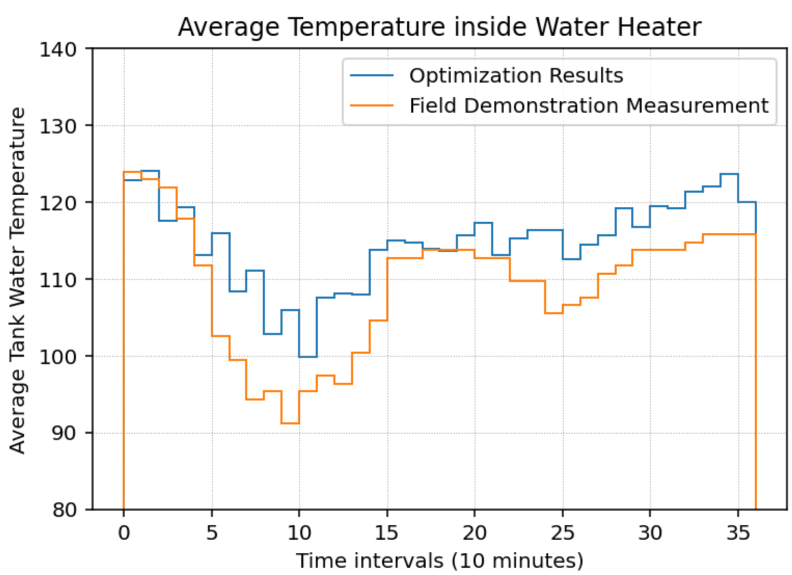

Figure 11. Comparison of the average tank water temperature between the optimized simulation case and the field deployment case.

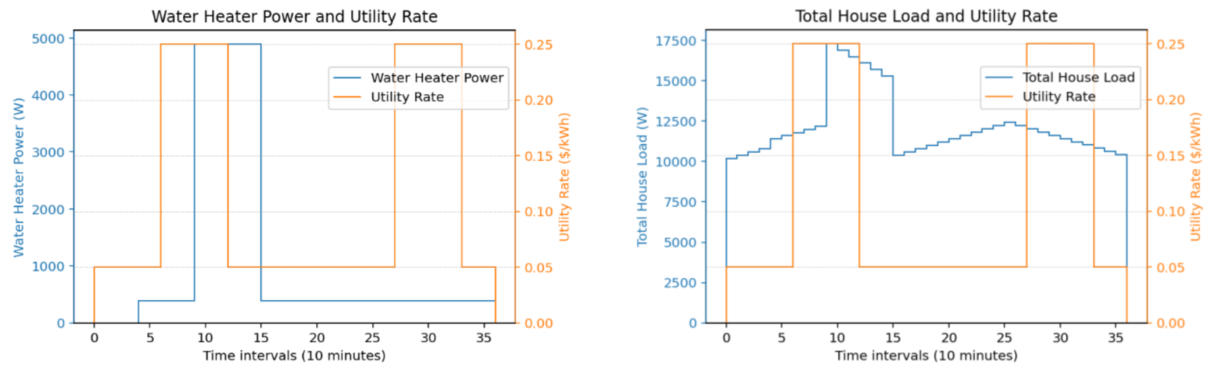

(a) (b)

Figure 12. Power consumption in the field deployment case of (a) the HPWH and (b) the total household.

Conclusions

A MILP-based optimization model to enable affordability by reducing the energy cost of operating water heaters is developed and described in this paper. The water heater is controlled by optimized selection of manufacture-defined operating modes rather than by directly turning the heating options on/off or by changing the temperature set points, thereby preserving consumers' privacy. Results of both numerical simulation and practical experiments validated the effectiveness of the proposed control.

From deployment, we learned several practical considerations that affect implementation: (1) model parameters and boundary conditions (ambient and inlet water temperature) can materially impact predicted temperatures, motivating calibration and periodic re-identification; (2) discrete mode selection reduces control granularity but improves deployability and privacy, and still provides meaningful flexibility because the tank acts as thermal storage; and (3) avoiding excessive mode switching is important to limit cycling and to align with device/communications constraints.

Future work will focus on improving robustness to uncertainty in hot-water draw and ambient conditions (e.g., stochastic/robust MPC or receding-horizon re-optimization), expanding the objective to include additional benefit to the utility and occupant, and evaluating performance across longer horizons, multiple households, and different utility tariffs. We also plan to assess scalability of the software framework for large scale coordination of building loads to quantify impacts on comfort metrics and equipment cycling over extended periods.

Acknowledgement

This material is based upon work supported by the U.S. Department of Energy, Office of Critical Minerals & Energy Innovation, Buildings Technologies Office, under contract number DE-AC05-000R22725.

Nomenclature

j	Index of nodes, running from 0 to N_N
t	Index of time periods, running from 0 to N_T
u_{tj}^{conv}	1 if thermal convection occurs and 0 otherwise

$M_t^{shed}, M_t^{normal}, M_t^{load}$	Binary mode indicators
$Chg_t^{shed}, Chg_t^{normal}, Chg_t^{load}$	Binary indicators of mode activation
Chg_t^{mode}	1 if mode changes and 0 otherwise
T_{tj}	Water temperature of node j during period t (°F)
T_t^{limit}	Lower temperature limit of dead band based on operating mode (°F)
P_t^T	Total household demand during period t (kW)
P^P	Peak household demand (kW)
$Q_{tj}^{cond}, Q_{tj}^{conv}$	Thermal conduction and convection of node j during period t (Btu)
$\overline{B_t^{HP}}, \underline{B_t^{HP}}$	Binary for heating control of heat pump, indicating upper/lower dead band is met
$\overline{B_t^{EE}}, \underline{B_t^{EE}}$	Binary for heating control of electric element, indicating upper/lower dead band is met
C_j	Thermal capacity of node j (Btu/°F)
W^C, W^M, W^P	Weighting factors
$D^{shed}, D^{normal}, D^{load}$	Temperature dead bands of modes (°F)
D^{on}, D^{off}	Temperature dead bands of electric element (°F)
λ_t	Electricity rate ($\$/kWh$)
A_j	Surface area of node j (m^2)
U	Tank wall heat transfer coefficient in $Btu/(h \cdot m^2 \cdot °F)$
T_t^A	Ambient air temperature during period t (°F)
T_t^C	Cold inlet water temperature during period t (°F)
T^{set}	Temperature setting of water heater (°F)
W_t	Hot water draw (gal/h)
c_p	Heat capacity of water in $Btu/(gal \cdot °F)$
ΔT^{max}	Maximum temperature difference between nodes (°F)
k	Thermal conductivity of water in $Btu/(h \cdot m \cdot °F)$
S	Surface area between nodes (m^2)
H^{HP}, H^{EE}	Heat of heat pump/electric element (Btu/h)
P^{HP}, P^{EE}	Power of heat pump/electric element (kW)
Δt	Time duration of each period (10 min)

References

Amasyali, K., J. Munk, K. Kurte, T. Kuruganti, and H. Zandi. 2021. "Deep Reinforcement Learning for Autonomous Water Heater Control." *Buildings* 11: 548. https://doi.org/10.3390/buildings11110548.

Ayoola, R. B., O. M. Ilori, N. Perera, M. Mateo-Garcia, K. Akinyemi, D. Boyd, and M. Leonard. 2025. "Data-Driven Optimisation of Residential Air-to-Water Heat Pump Performance Using IoT and Machine Learning." *Energy and Buildings* 348: 116352.

Bursill, J., and C. A. Cruickshank., 2015. “Heat Pump Water Heater Control Strategy Optimization for Cold Climates.” ASME. *J. Sol. Energy Eng.* 138(1): 011011. https://doi.org/10.1115/1.4032144

Clift, D. H., C. Stanley, K. N. Hasan, and G. Rosengarten. 2023. “Assessment of Advanced Demand Response Value Streams for Water Heaters in Renewable-Rich Electricity Markets.” *Energy* 267: 126577.

COIN-OR. 2022. “CBC User Guide.” https://www.coin-or.org/Cbc/cbcuserguide.html (accessed on December 21, 2025).

Energy Information Administration. 2009. “Residential energy consumption survey: 2009.” Washington, D.C.: EIA.

Grant, P., M. Stübs, B. Nordman, and C. Gehbauer. 2023. “Stabilizing the Grid and Reducing Utility Bills Through Price-Responsive Controls for Heat Pump Water Heaters,” in 2023 ASHRAE Summer Conference.

Hall, J., M. Starke, J. Munk, H. Zandi, T. Kuruganti, and H. Buckberry. 2022. “A System of Agents for Supporting Optimization and Control of a Connected Community.” *IEEE Journal of Emerging and Selected Topics in Industrial Electronics* 3(1): 57–68.

Jin, X., J. Maguire, and D. Christensen. 2014.“Model Predictive Control of Heat Pump Water Heaters for Energy Efficiency.” *Proceedings of the 18th ACEEE Summer Study on Energy Efficiency in Buildings*: 21–26. Pacific Grove, CA: ACEEE.

Liu, Y., and B. Yildiz. 2025. “Techno-Economic Optimization of Electric Water Heater and Battery Energy Storage for Residential Dwellings with Rooftop PV Systems.” *Energy and Buildings* 342: 115856.

Mande, C., A. Aboud, L. dela Rosa, R. Collins, and M. Ellis. 2022. “Timing is Everything: Optimizing Load Flexibility of Heat Pump Water Heaters for Cost, Comfort, and Carbon Emissions.” UC Davis.

Pardiñas, Á. Á., P. D. Gómez, F. E. Camarero, and P. C. Ortega. 2023. “Demand–Response Control of Electric Storage Water Heaters Based on Dynamic Electricity Pricing and Comfort Optimization.” *Energies* 16(10): 4104. https://doi.org/10.3390/en16104104.

Shad, M., A. Momeni, R. Errouissi, C. P. Diduch, M. E. Kaye, and L. Chang. 2017. “Identification and Estimation for Electric Water Heaters in Direct Load Control Programs.” *IEEE Transactions on Smart Grid* 8(2): 947–955.

Smith, Robert, Liu, Yan, Lupo-Pasini, Massimiliano, Yoon, Yeobeom, and Zandi, Helia. 29 Aug. 2025. ACTIVE. Computer Software. https://github.com/SmithRWORNL/ACTIVE. USDOE Office of Energy Efficiency and Renewable Energy (EERE), Energy Efficiency Office. Building Technologies Office. Web. doi:10.11578/dc.20260216.1.

Starke, M., J. Munk, H. Zandi, T. Kuruganti, H. Buckberry, J. Hall, and J. Leverette. 2020. "Real-Time MPC for Residential Building Water Heater Systems to Support the Electric Grid." *2020 IEEE Power & Energy Society Innovative Smart Grid Technologies Conference (ISGT)*: 1–5. Washington, DC: IEEE.

Stübs, M., P. Grant, and B. Nordman. 2024. "Demonstrating Load-Shaping Capabilities of Cost Minimizing Heat Pump Water Heater Controls with Varying Price Profiles." *2024 IEEE Power & Energy Society General Meeting (PESGM)*: 1–5.

Tsybina, E., C. Winstead, J. Hill, K. Amasyali, N. Agah, V. Lebakula, J. Munk, and H. Zandi. 2023. "Peak Reduction Using Mode Adjustment of Heat Pump Water Heaters in a Residential Neighborhood." *2023 IEEE PES Innovative Smart Grid Technologies Latin America (ISGT-LA)*: 455–459. San Juan, Puerto Rico: IEEE.